

Continuous-variable entanglement dynamics in Lorentzian environment

Berihu Teklu

Department of Applied Mathematics and Sciences, Center for Cyber-Physical Systems (C2PS), Khalifa University, Abu Dhabi 127788, United Arab Emirates

Abstract

We address the non-Markovian entanglement dynamics for bimodal continuous variable quantum systems interacting with two independent structured reservoirs. We derive an analytical expression for the entanglement of formation without performing the Markov and the secular approximations. We observe a variety of qualitative features such as entanglement sudden death, dynamical generation, and protection for two types of Lorentzian spectral densities, assuming the two modes initially excited in a twin-beam state. Our quantitative analysis shows that these cases with different reservoir spectrum, the environmental temperature and the initial amount of entanglement differ significantly in these qualitative features.

1. Introduction

Recent advances in the study of the evolution of entanglement for open quantum systems is an important issue for both fundamental and practical reasons, as quantum entanglement is an essential resource for quantum information processing [1, 2]. The properties of open systems play an essential role in determining how the observed classical world emerges from its quantum mechanical underpinnings via the process known as decoherence. Any realistic analysis of quantum information protocols should take into account the decoherence effect of the environment. In order to realize the promise of a quantum information processor, the inevitable decoherence-inducing effect of any system-environment interaction must be taken into account. The time scales on which these processes take place and strategies to reduce these effects are a major topic of research. Therefore, in order to describe the dynamics of the system of interest, the theoretical results strongly depend on the underlying dissipative dynamics and the performed approximations. Within the theory of open quantum systems, the dissipative dynamics are mainly described by master equations of the reduced density matrix. The most relevant Born-Markov approximation assumes weak coupling between the system and the environment to justify a perturbative treatment and neglects short-time correlations between the system and the reservoir. This approach has been widely and successfully employed in the field of quantum optics [3] where the characteristic time scale of the en-

vironmental correlations is much shorter compared to the internal system dynamics. There are a few cases, however, where an exact analytical description of the dynamics is possible. Two relevant examples are the quantum Brownian motion (QBM) [4, 5, 6, 7, 8] and the case of a two-level atom interacting with a zero-temperature reservoir with Lorentzian spectral density [4, 9, 10, 11, 12, 13, 14].

Any physical operations that reflects the time evolution of the state of a quantum system can be regarded as a channel. In particular, quantum channels grasp the way how quantum states are modified when subjected to noisy quantum communication lines. Couplings to other external degree of freedom, often beyond detailed control, will typically lead to losses and decoherence, effects that are modeled by appropriate non-unitary quantum channels.

Quantum entanglement in continuous variables (CV) quantum channels has been considered as a key resource in many aspects and applications of quantum information processing due to potential improvement in the channel capacity [15]. In the real world, the quantum coherence and entanglement of a quantum system will inevitably be influenced and degraded by the external environment. There are several investigations in the analysis of CV channels in the description of noisy CV quantum channels taking into account decoherence and dissipation phenomena [16]. In those investigations, the Markovian approximations or/and the rotating wave approximations (RWA) is/are assumed. However, if a

short time interval or regime, comparable with the environment correlation time, is concerned, or if the environment is structured with a particular spectral density, then non-Markovian environment effect could become significant. For example, for high-speed quantum communication where the characteristic time scales become comparable with the reservoir correlation time.

Challenged by new experimental evidence a growing interest in non-Markovian descriptions has developed. From some phenomenological [17, 18] and microscopic models [19, 20, 21, 22, 23] of non-Markovian quantum channels have been proposed. Entanglement dynamics for such kinds of systems was analyzed before and a variety of results available. It was shown that the environment may completely disentangle an initial entangled state [19, 24, 25].

A few theoretical proposals advance the entanglement dynamics in noisy continuous variable (CV) [26]: most generally the interaction between the system-reservoir and a structured environment, where the system-reservoir correlations persist long enough to require a non-Markovian treatment, even in the weak coupling limit [19, 27, 28, 29, 31]. Besides its own importance from a theoretical point of view, the role of structured environments and non-Markovianity in quantum metrology [32, 33, 34, 35, 36, 37, 38, 39], quantum key distribution [40], and channel capacities [41], showing that non-Markovian quantum channels may be advantageous compared to Markovian ones. The theory developed in this article is relevant to the evolution of entanglement in bimodal continuous variable quantum systems interacting with two independent structured reservoirs. In this paper, we will analyze the entanglement dynamics using an analytic expression for the evolution of the entanglement of formation (EOF) [42, 43, 44]. We assume the two oscillators initially excited in a twin-beam state (TWB). Despite its great simplicity, these models allow to describe the transition between Markovian and non-Markovian dynamics in experimental realization [45, 46]. By considering a Lorentzian environment we are able to obtain the exact reduced dynamics by means of the pseudomode method.

The outline of this article is as follows: in Sec. 2, we describe our model and present the non-Markovian master equation. Section 3 presents an overview about two-mode Gaussian states and the solution of the master equation with an initial Gaussian state. In addition, we present the concept of EOF for two-mode CV Gaussian state. In Sec. 4 we describe cases where entanglement meets entanglement sudden death (ESD) and identify conditions or parameters where entanglement can survive, some for ever - “always alive” (AL). Finally, in

Sec. 5 we conclude with a summary and outlook.

2. Effective Master Equation and Weak Coupling

The focus of our analysis is the non-Markovian dynamics of a system of two identical non-interacting quantum harmonic oscillators, each of them coupled to its own bosonic structured reservoir, giving rise to the total Hamiltonian

$$H = \sum_{j=1,2} \hbar\omega_0 a_j^\dagger a_j + \sum_{j=1,2} \sum_k \hbar\omega_{jk} b_{jk}^\dagger b_{jk} + \sum_{j=1,2} \sum_k \gamma_{jk} (a_j + a_j^\dagger) (b_{jk} + b_{jk}^\dagger). \quad (1)$$

In this Hamiltonian the first, second and third terms describe the system, environment and interaction, respectively, with $a_j(a_j^\dagger)$ and $b_{jk}(b_{jk}^\dagger)$ being the annihilation (creation) operators of the system and reservoirs harmonic oscillators, respectively. ω_0 the oscillators frequency, ω_{1k} and ω_{2k} the frequencies of the reservoirs modes, and γ_{jk} the coupling between the j -th oscillator and the k -th mode of its environment. In the following we assume that the reservoirs have the same spectrum and are equally coupled to the oscillators.

The problem of a quantum harmonic oscillator interacting with a bosonic reservoir in thermal equilibrium has been derived for the first time in Ref. [8], and it is usually referred to as Hu-Paz-Zhang Master equation. The exact non-Markovian master equation for the bimodal field interacts bilinearly with two identical uncorrelated bosonic thermal reservoirs takes the form [19]

$$\dot{\rho}(t) = \sum_k \left\{ \frac{1}{i\hbar} [H_k^0, \rho(t)] - \Delta(t) [X_k, [X_k, \rho(t)]] + \Pi(t) [X_k, [P_k, \rho(t)]] + \frac{i}{2} r(t) [X_k^2, \rho(t)] - i\gamma(t) [X_k, \{P_k, \rho\}] \right\}, \quad (2)$$

where

$$X_k = \frac{1}{\sqrt{2}} (a_k + a_k^\dagger) \quad P_k = \frac{i}{\sqrt{2}} (a_k^\dagger - a_k)$$

are the dimensionless quadrature operators. The operators \hat{a}^\dagger and \hat{a} are the creation and annihilation operators of the two oscillators and $H_k^0 = \hbar\omega_0(a_k^\dagger a_k + 1/2)$. These operators satisfy the bosonic commutation relation $[a_k, a_k^\dagger] = 1$ ($k = 1, 2$). We see that the Master equation given by Eq. (2), while it is exact, it describes also the non-Markovian system-reservoir correlations

due to the finite correlation time of the reservoir. All the non-Markovian character of the system is contained in the time dependent coefficients, $\Delta(t)$, $\Pi(t)$, $r(t)$ and $\gamma(t)$, appearing in the Master equation. These coefficients depend only on the reservoir spectral density, that is, on the microscopic effective coupling strength between the system oscillator and the oscillators of the reservoir. The coefficient $r(t)$ describes a time dependent frequency shift, $\gamma(t)$ is the damping coefficient, $\Delta(t)$ and $\Pi(t)$ are the normal and the anomalous diffusion coefficients, respectively [4, 7]. It is worth noting that the Master equation given by Eq. (2) is valid for general forms of the reservoir spectral density $J(\omega)$ and any temperature T . These time dependent coefficients are expressed in terms of series expansions in the system-reservoir coupling constant α . Demanding weak system-reservoir couplings, that is, fulfilling the condition $\alpha \ll 1$, one can stop the expansion to the second order in the coupling constant and obtain analytic solutions for the coefficients. The analytic expression are given in the Appendix for the both low and high temperature-reservoirs characterized by a spectral densities of the form (11) and (12) respectively.

The method is based on the quantum characteristic approach [47] in which the solution of the master equation (2) may be written as

$$\chi_t(\Lambda) = e^{-\Lambda^T [\bar{W}(t) \oplus \bar{W}(t)] \Lambda} \times \chi_0(e^{-\Gamma(t)/2} [R^{-1}(t) \oplus R^{-1}(t)] \Lambda), \quad (3)$$

where $\chi_t(\Lambda)$ is the characteristic function at time t , χ_0 is the characteristic function at the initial time $t = 0$, $\Lambda = (x_1, p_1, x_2, p_2)$ is the two-dimensional phase space variables vector, $\Gamma(t) = 2 \int_0^t \gamma(t') dt'$, and $\bar{W}(t)$ and $R^{-1}(t)$ are 2×2 matrices. The former matrix is given by

$$\bar{W}(t) = e^{-\Gamma(t)} [R^{-1}(t)]^T W(t) R^{-1}(t), \quad (4)$$

while the latter one, $R(t)$, contains rapidly oscillating terms. In the weak coupling limit $R(t)$ takes the form

$$R(t) = \begin{pmatrix} \cos \omega_0 t & \sin \omega_0 t \\ -\sin \omega_0 t & \cos \omega_0 t \end{pmatrix}. \quad (5)$$

Finally, $W(t) = \int_0^t e^{\Gamma(s)} \bar{M}(s) ds$ with $\bar{M}(s) = R^T(s) M(s) R(s)$ and

$$M(s) = \begin{pmatrix} \Delta(s) & -\Pi(s)/2 \\ -\Pi(s)/2 & 0 \end{pmatrix}. \quad (6)$$

3. Entanglement dynamics for Gaussian states

After the description of the master equation and its general solution through the characteristic function approach, we move on to a detailed analytic solution for

the characteristic function in the weak coupling limit obtained in [47]. Note first that the initial state of the subsystem is taken of Gaussian form and the evolution induced by the master equation (2) under the quantum dynamical semigroup assures the preservation in time of the Gaussian form of the state. In order to evaluate the EOF for the two modes initially excited in a TWB state, we can obtain the expression of the covariance matrix at time t .

3.1. Analytic solution in the weak coupling limit

We consider a two-mode Gaussian states, that is, those states characterized by a Gaussian characteristic function $\chi_0(\Lambda) = \exp\{-\frac{1}{2} \Lambda^T \sigma_0 \Lambda - i \Lambda^T \bar{\mathbf{X}}_{in}\}$, where σ_0 the initial covariance matrix

$$\sigma_0 = \begin{pmatrix} \mathbf{A}_0 & \mathbf{C}_0 \\ \mathbf{C}_0^T & \mathbf{B}_0 \end{pmatrix}, \quad (7)$$

where $\mathbf{A}_0 = a \mathbb{1}$, $\mathbf{B}_0 = b \mathbb{1}$, $\mathbf{C}_0 = \text{Diag}(c_1, c_2)$, and $a = b = \cosh(2r)$ and $c_1 = -c_2 = \sinh(2r)$ with $r > 0$, and $\mathbb{1}$ the 2×2 identity matrix.

Similar to Ref. [27] the interaction between oscillators and baths is bilinear in position and momentum, thus the evolution maintains the Gaussian character. The evolved state is a two-mode Gaussian state with mean and covariance matrix are described by

$$\bar{\mathbf{X}}_t = e^{-\Gamma(t)/2} (R \oplus R) \bar{\mathbf{X}}_{in} \quad (8)$$

$$\sigma_t = e^{-\Gamma(t)} (R \oplus R) \sigma_0 (R \oplus R)^T + 2(\bar{W}_t \oplus \bar{W}_t), \quad (9)$$

Using the weak coupling approximations described in Eqs. (3)–(6) and replacing the matrix \bar{W}_t , the covariance matrix at time t is now given by

$$\sigma_t = \begin{pmatrix} A_t & C_t \\ C_t^T & A_t \end{pmatrix}. \quad (10)$$

The analytic expression of the matrices A_t and C_t is given in the in the Appendix for both low and high temperature-reservoirs.

In order to study in more details the entanglement dynamics in a non-Markovian channel, we need to specify the properties of the bosonic reservoirs. As a first model of the environment for the case of zero temperature Lorentzian spectral density has takes the form

$$J(\omega) = \frac{1}{\omega^2 + \lambda^2}, \quad (11)$$

The parameter λ represents the width of the distribution, which is connected to the reservoir correlation time. In this model, the reservoir correlation time is given by the

inverse of the system-reservoir interactions time, that is, $\tau_R = 1/\lambda$. In order to make a comparative study, we could deal with any given form of the spectral density. But as a particular example, we use the following form of spectral density to specify the environments at high temperature and the spectral density is of the form

$$J(\omega) = \frac{\omega}{\omega^2 + \lambda^2}. \quad (12)$$

The physical meaning when viewing the Lorentzian spectral density (12) as a mathematical vehicle to conveniently model a non-zero temperature bath correlation function with microscopically defined spectral density. We also concentrate on a particular class of entangled initial states, i.e. the TWB vacuum states, obtained by applying the two mode squeezing operator $S(\zeta) = \exp(\zeta a^\dagger b^\dagger - \zeta^* ab)$ to the vacuum state of the two modes, with $\zeta = re^{i\phi}$. The TWB state is thus determined only by the squeezing parameter r which also determines the initial amount of entanglement. Analytic expressions for the relevant time dependent coefficients given in Eq. (A.1) can be derived by approximating in the high- T and zero- T limits, that is, for $2N(\omega) + 1 \approx \frac{2k_B T}{\hbar\omega}$ and $2N(\omega) + 1 \approx 1$, respectively (The mathematical steps are outlined in Appendix A).

3.2. Entanglement of Formation

Entangled two-mode Gaussian states are a key resource for quantum technologies such as quantum cryptography, quantum computation and teleportation, so quantification of Gaussian entanglement is an important problem. A convenient and proper way of measuring quantum correlations in CV systems is by means of EOF [42, 43]. EOF quantifies the minimum amount of two-mode squeezing needed to prepare an entangled state from a classical one. However, an analytical expression for EOF exists only for special cases, e.g., for two qubits [48] and for an arbitrary bimodal Gaussian state [44] and finding a closed formula for an arbitrary state remains an open problem to this day. For simplicity, we will assume that the initial state is a symmetric bipartite Gaussian state with covariance matrix given by Eq. (7). As we mentioned above, when this state interacts with two identical independent reservoirs, the action of a Gaussian operation (any operation that transforms a Gaussian state into another Gaussian state) and the evolved covariance matrix is given by Eq. (10). The EOF for all symmetric Gaussian states corresponding to two modes is given by [43]

$$E_F = (x_m + \frac{1}{2}) \ln(x_m + \frac{1}{2}) - (x_m - \frac{1}{2}) \ln(x_m - \frac{1}{2}), \quad (13)$$

with $x_m = (\tilde{\kappa}_-^2 + 1/4)/(2\tilde{\kappa}_-)$, $\tilde{\kappa}_- = \sqrt{(a_n - c_+)(a_n - c_-)}$ being the minimum symplectic eigenvalue of the CM σ_t , and

$$a_n = \sqrt{I_1}, \quad (14)$$

$$c_{\pm} = \sqrt{\frac{I_1^2 + I_3^2 - I_4 \pm \sqrt{(I_1^2 + I_3^2 - I_4)^2 - (2I_1 I_3)^2}}{2I_1}}, \quad (15)$$

where $I_1 = \det[A_t]$, $I_3 = \det[C_t]$ and $I_4 = \det[\sigma_t]$ are the symplectic invariants of σ_t .

4. The entanglement dynamics

Entanglement is not only a property of quantum mechanics but also of a crucial resource that allows certain quantum protocols to be more efficient than their classical counterpart [1, 2]. However, the inevitable interaction between the quantum system and its environments leads to loss of entanglement. Studying this sort of model led to the discovery of the entanglement sudden death (ESD) phenomenon in which the entanglement between two qubits decays to zero in a finite time rather than asymptotically, has been predicted theoretically [49] and subsequently been verified experimentally [50], indicating specific behavior of entanglement that differs from that of coherence. Reference [51] found that the entanglement can revive after some time interval of ESD and thus extends significantly the entangled time of the qubits. This remarkable phenomenon, which has been experimentally observed [52], is physically due to the dynamical back action (that is, the non-Markovian effect) of the memory environments [51, 53]. However, in many cases the finite extension of the entangled time is not enough and thus it is desired to preserve a significant fraction of the entanglement in the longtime limit. Indeed, it has shown [54] that some noticeable fraction of entanglement can be obtained by engineering structured environment such as a photonic bandgap materials [55, 56, 57].

In order to investigate the decoherence effect in the entanglement dynamics induced by the environment, a specification of the spectral density $J(\omega)$ of the environment is required. We have briefly investigated the parameters influencing the time evolution are the reservoir temperature, the form of the reservoir spectrum and the supporting mode ω_0 , resulting from the combination of the reservoir spectrum. We will study the effect of these parameters separately in the following dealing with the dynamics for $T = 0$, for high- T reservoirs, and

a comparison with different reservoir spectra. We are also interested in finding the influence of how the initial state of the system, in particular, on the initial squeezing parameter r of TWBs on the validity of the secular approximation.

An interesting problem in this context, is entanglement dynamics for various types of structured reservoirs and for different reservoir temperatures. It is well known from previous studies on open quantum systems that interacting with zero-temperature reservoirs we expect on the one hand slowing down the loss of entanglement [58] and on the other hand more pronounced the non-Markovian features [59], with respect to the $T \neq 0$ case.

To address this problem, we now proceed with a reservoir of the form (11) at zero temperature Lorentzian bath with $\omega_0 = 5$ and look at the dynamics of a TWB with a different amount of initial entanglement, r . In Fig. 1 (left panel), we show an example of entanglement evolution characterized by oscillations, sudden death and revivals. Fig. 1 (right panel), shows that the evolution of the entanglement persist longer for a longer time at $r = 0.2$ and appear oscillations even as the state approaches the ground state. As one would expect, the exact and the secular approximated dynamics completely agree in this situation. We have also carefully examined the dynamical behavior for other chosen parameters of ω_0 and of the initial squeezing parameter r , we observe that there is quite general property of the system. Therefore, for a general description of bimodal CV quantum systems interacting with zero temperature reservoirs, the secular approximation can always be performed well and we always neglect the effects of the nonsecular terms. We realize from this that the secular terms (B.1) are temperature dependent through the diffusion coefficients $\Delta(t)$ and $\Pi(t)$, and at $T = 0$ their contribution is rather small.

For intermediate values of the parameter ω_0 , $\omega_0 \leq 1$, we observe a stronger dependence on the initial value of the entanglement. In Fig. 2, we plot the time evolution of the EOF for the entanglement dynamics calculated using the secular approximated solution and the exact solution for two different initial TWB states. For a range of higher values of the initial entanglement, the entanglement dynamics are robust to decoherence.

In the same way as above, we consider the high-temperature limit $k_B T \gg \hbar \omega_0$, that is, when the classical thermal energy $k_B T$ is much larger than the typical energies exchanged in our system. In the following analysis we choose a temperature such that $k_B T / \hbar = 100$, thus we can examine scenarios in which $\omega_0 \geq 0.1$.

It will turn out that the behavior of the time evolution

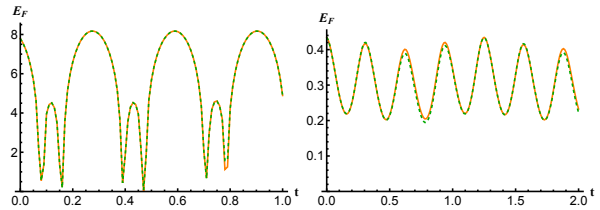


Figure 1: (Colors online) Dynamics of exact EoF (solid red line) and the secular approximate (dashed blue line) as a function of t , for the Lorentzian spectral density model (11) at zero temperature for $\alpha = 0.1$, $\lambda = 0.1$, with $\omega_0 = 5$, (a) $r = 2$ and (b) $r = 0.2$. The two curves almost overlap perfectly.

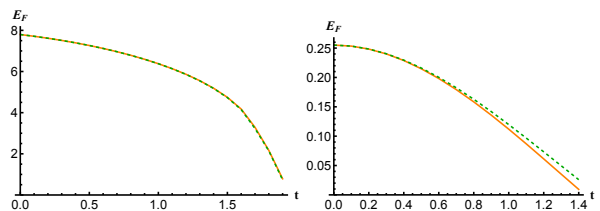


Figure 2: (Colors online) The exact EoF (solid orange line) and the secular approximate dynamics (dashed green line) of the E_F as a function of t , for the Lorentzian spectral density model (11) at zero temperature for $\alpha = 0.1$, $\lambda = 0.1$, with $\omega_0 = 0.2$, (a) $r = 2$ and (b) $r = 0.1$. The two curves almost overlap perfectly for higher values of squeezing.

of entanglement in CV quantum channels in the class of Ohmic-like spectral distribution with an exponential cutoff function has been studied in detail in [27]. We can however summarize the most important features for the non-Markovian short time dynamics of entanglement in CV quantum channels in the case of the spectral distribution of the form (12) and $\omega_0 = 10$. In Fig. 3, we plot the important features of the time evolution of the EOF calculated using both the secular approximated solution and the exact solution in the regime $\omega_0 \geq 1$ for two different initial TWB states. Figure 3 (left panel) shows that for higher values of the initial entanglement, that is, for larger values of r , the entanglement dynamics exhibits the behavior of oscillations. For small initial entanglement ($r = 0.01$), where the entanglement dynamics is significantly changed as we see from Fig. 3 (right panel). One may also see that the exact and the secular approximated dynamics sensibly agree for $r = 2$ (higher initial entanglement) during the initial time but fails after $t \geq 0.1$ and for small value of the initial entanglement $r = 0.01$, the secular approximation does not work well. Furthermore, both the secular approximation and the exact results show oscillations for higher values of the initial entanglement as clearly visible in the dynamics. From previous study [27], one would have conclude that the entanglement dynamics in the high tem-

perature case is affected by the secular approximation. Our results, however, clearly show on the contrary that the entanglement dynamics at high temperature and for smaller values of initial entanglement, the secular terms predicts much longer disentanglement time.

Having analyzed the differences in the entanglement dynamics for values of the parameters $\omega_0 \geq 1$, we now focus on the intermediate values of the parameters ω_0 , $\omega_0 \leq 1$, we observe a strong dependence on the initial value entanglement. In Fig. 4, we study the dependence of the initial value entanglement and shows that for both initial conditions the entanglement oscillations are strongly suppressed. As one would expect, the secular approximations for the high- T dynamics affected by this approximation. On the other hand, for both initial values of the entanglement the amplitude of the secular approximations increases.

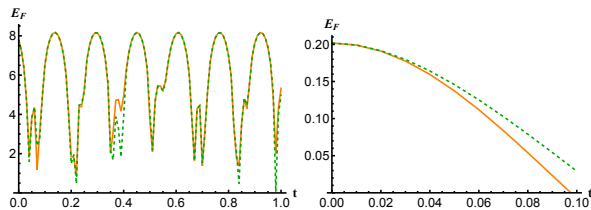


Figure 3: (Colors online) Comparison between the exact EoF dynamics (solid orange line) and the secular approximate dynamics (dashed green line) as a function of t , with $\omega_0 = 10$, (a) $r = 2$ and (b) $r = 0.01$. We set $k_B T / \hbar = 100$, $\lambda = 0.1$, $\alpha = 0.1$.

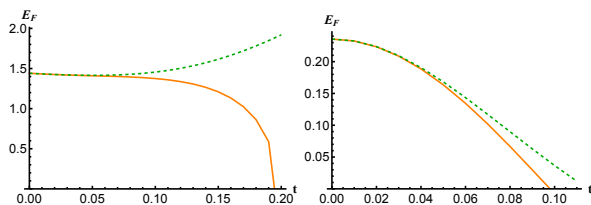


Figure 4: (Colors online) Dynamics of the exact EoF dynamics (solid orange line) and the secular approximate dynamics (dashed green line) as a function of t , with $\omega_0 = 0.15$, (a) $r = 1$ and (b) $r = 0.08$. We set $k_B T / \hbar = 100$, $\lambda = 0.1$, $\alpha = 0.1$.

So far, we have studied the entanglement dynamics, as measured by the entanglement of formation, for the two modes initially excited in a TWB for a single Lorentzian spectral distribution of the form given in (11) and (12). The phenomenon of entanglement sudden death has clearly provoked much theoretical interest, and it is related to another question that is both interesting from a theoretical perspective and clearly of great practical importance: how can one protect a system from disentanglement? Here we do not propose any active

scheme for protecting entanglement but rather consider what initial amount of entanglement and the ranges of ω_0 tend to minimize the loss of entanglement or safeguard entanglement once it has been dynamically generated. Of particular interest is avoiding ESD. Another intriguing aspect is now how the entanglement preservation is influenced by the effect of temperature on the non-Markovian dynamics. As shown in Figure (4), we sharply note that the exact solution containing the non-secular terms exhibits ESD. On one hand, the disentanglement time predicted by the exact and secular results increases with increasing values of initial entanglement, that is, for larger values of r . Meanwhile, the entanglement oscillations is sustained for the longest time for higher values of the initial entanglement. Finally, as shown in Figure (1), we investigate the effects of higher value of ω_0 for different values of initial entanglement. It is interesting to note that the time evolution of the entanglement dynamics has significant differences for different values of initial entanglement r . For a range of small values of r , one can clearly see that the entanglement exhibits the behavior of oscillation and is sustained for longer time. Also in this case one can clearly see that the exact and secular approximated dynamics sensibly agree. We should mention that the entanglement oscillations have also been found for two uncoupled harmonic oscillators interacting with two independent reservoirs [19]. In the following, we investigate the difference in the loss of entanglement due to the choice of the amount of entanglement in the initial TWB state, given by the value of squeezing parameter r and due to different reservoir spectra. We have seen that the non-Markovian revivals of entanglement occur for intermediate value of the squeezing parameter r (right panel in the high- T limit) and with the state being AL (left panel for the zero- T case). In all cases there are entanglement oscillations and ESD, while an entanglement revival is also present for higher values of ω_0 and the initial amount of entanglement r .

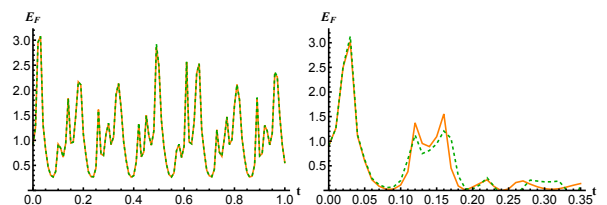


Figure 5: (Colors online) Dynamics of the exact EoF dynamics (solid orange line) and the secular approximate dynamics (dashed green line) as a function of t , with $\omega_0 = 10$, $r = 0.6$ for the Lorentzian environment reservoir of the form (11) (Left) and for the high- T limit (12). We set $k_B T / \hbar = 100$, $\lambda = 0.1$, $\alpha = 0.1$.

5. Summary and outlook

In the present work, we have studied the entanglement dynamics in a model consisting of two different Lorentzian spectral densities in non-Markovian environments as measured by the entanglement of formation, for the two modes initially excited in a twin-beam state in terms of phenomena such as dynamical entanglement generation, entanglement sudden death, and an “always alive” (AL) phenomenon where entanglement once present never goes to zero at any time. A similar work has also been studied the evolution of entanglement in bimodal continuous variable quantum systems with two independent structure reservoir in thermal equilibrium [19, 27, 28].

We investigated the entanglement dynamics as a function of the reservoir spectrum, the temperature and the initial amount of entanglement. In our first Lorentzian bath (11), we considered higher values of ω_0 in the zero-temperature case showed that the evolution of the entanglement persists longer for a longer time and appear oscillations for intermediate values of the initial entanglement. Moreover, for $\omega_0 < 1$, the entanglement dynamics are completely robust against decoherence. Note also that the secular and exact dynamics almost coincide for higher initial entanglement. In the second Lorentzian model (12) at high-temperatures we see that the non-Markovian entanglement oscillations persists for longer time for higher values of the initial entanglement. We also see from Fig. 3 (right panel) that the exact solution in the high- T dynamics has a shorter disentanglement time. At high-temperature and intermediate values of the parameters $\omega_0 < 1$, ESD appears for each value of the initial entanglement for the exact dynamics and entanglement predicts longer for the secular solutions. We also find that entanglement is more robust in the case of zero-temperature Lorentzian bath while it vanishes faster for the high-temperature Lorentzian bath. Also Gaussian entanglement oscillations [19] are evident for the higher values of the reservoir spectrum and intermediate value of the squeezing parameter, a result independent, qualitatively, on the temperature of the bath.

Recently, there have been a lot of interest in the entanglement dynamics in CV quantum channels, both for common and independent reservoirs. The result presented in this article demonstrate that careful manipulation of the non-Markovian short time dynamics of entanglement in different physical scenarios. This means that, in certain situations, the effects of different reservoirs on the time evolution of entanglement in CV quantum channels, with the potential to pave the way to real-

scale quantum-enhanced devices [41].

Acknowledgments

I would like to acknowledge Matteo Paris and Stefano Olivares for helpful discussions. This work has been supported by Khalifa University through project no. 8474000358 (FSU-2021-018).

Appendix A. Time dependent coefficients at the second order in α

The time-dependent coefficients of the master equation given in (2), in the case of thermal reservoirs in the weak coupling regime ($\alpha \ll 1$) are given by

$$\Delta(t) = \alpha^2 \int_0^t ds \int_0^{+\infty} d\omega J(\omega) [2N(\omega) + 1] \cos(\omega s) \cos(\omega_0 s), \quad (\text{A.1a})$$

$$\Pi(t) = \alpha^2 \int_0^t ds \int_0^{+\infty} d\omega J(\omega) [2N(\omega) + 1] \cos(\omega s) \sin(\omega_0 s), \quad (\text{A.1b})$$

$$\gamma(t) = \alpha^2 \int_0^t ds \int_0^{+\infty} d\omega J(\omega) \sin(\omega s) \sin(\omega_0 s), \quad (\text{A.1c})$$

$$r(t) = \alpha^2 \int_0^t ds \int_0^{+\infty} d\omega J(\omega) \sin(\omega s) \cos(\omega_0 s), \quad (\text{A.1d})$$

where $N(\omega) = [\exp(\hbar\omega/k_B T) - 1]^{-1}$ is the mean number of photons with frequency ω , and α is the dimensionless system-reservoir coupling constant, while $J(\omega)$ defines the spectral distribution of the environment.

For the Lorentzian spectral density of the form $J(\omega) = \frac{1}{\omega^2 + \lambda^2}$, in the low T limit ($2N(\omega) + 1 \approx 1$) and we made use of the following special mathematical functions [60]:

$$\text{Ei}(z) = - \int_{-z}^{+\infty} \frac{e^{-t}}{t} dt \quad \text{Si}(z) = \int_0^z \frac{\sin t}{t} dt.$$

$$\begin{aligned} \gamma(t) = \frac{\alpha^2}{\omega_0^2 + \lambda^2} \left\{ \left(\text{Si}(\omega_0 t) \right. \right. & \quad (\text{A.2}) \\ & + \frac{\pi}{2} \left. \right) + \frac{1}{2} \frac{\omega_0}{\lambda} \cos(\omega_0 t) \left(e^{\lambda t} \text{Ei}(-\lambda t) - e^{-\lambda t} \text{Ei}(\lambda t) \right) \\ & - \frac{1}{2} \sin(\omega_0 t) \left(e^{\lambda t} \text{Ei}(-\lambda t) + e^{-\lambda t} \text{Ei}(\lambda t) \right) \left. \right\} \end{aligned}$$

$$\Delta_0(t) = \frac{\pi\alpha^2}{2(\omega_0^2 + \lambda^2)} \left\{ e^{-\lambda t} \left(\frac{\omega_0}{\lambda} \sin(\omega_0 t) - \cos(\omega_0 t) \right) + 1 \right\} \quad (\text{A.3})$$

$$\Pi_0(t) = \frac{\pi\alpha^2}{2(\omega_0^2 + \lambda^2)} \left\{ \frac{\omega_0}{\lambda} \left(1 - \cos(\omega_0 t) e^{-\lambda t} \right) - \sin(\omega_0 t) e^{-\lambda t} \right\} \quad (\text{A.4})$$

For the Lorentzian spectral density of the form $J(\omega) = \frac{\omega}{\omega^2 + \lambda^2}$ in the high- T limit ($2N(\omega) + 1 \approx \frac{2k_B T}{\hbar\omega}$), we have

$$\begin{aligned} \gamma(t) = & \frac{\alpha^2 \beta}{\omega_0^2 + \lambda^2} \left\{ \left(\text{Si}(\omega_0 t) + \frac{\pi}{2} \right) \right. \\ & + \frac{1}{2} \frac{\omega_0}{\lambda} \cos(\omega_0 t) \left(e^{\lambda t} \text{Ei}(-\lambda t) - e^{-\lambda t} \text{Ei}(\lambda t) \right) \\ & \left. - \frac{1}{2} \sin(\omega_0 t) \left(e^{\lambda t} \text{Ei}(-\lambda t) + e^{-\lambda t} \text{Ei}(\lambda t) \right) \right\} \quad (\text{A.5}) \end{aligned}$$

$$\Delta_T(t) = \frac{\pi\alpha^2\beta}{2(\omega_0^2 + \lambda^2)} \left\{ e^{-\lambda t} \left(\frac{\omega_0}{\lambda} \sin(\omega_0 t) - \cos(\omega_0 t) \right) + 1 \right\} \quad (\text{A.6})$$

$$\Pi_T(t) = \frac{\pi\alpha^2\beta}{2(\omega_0^2 + \lambda^2)} \left\{ \frac{\omega_0}{\lambda} \left(1 - \cos(\omega_0 t) e^{-\lambda t} \right) - \sin(\omega_0 t) e^{-\lambda t} \right\} \quad (\text{A.7})$$

We do not provide the analytic expression of $r(t)$ because its contribution is negligible to the solution in the weak coupling limit.

Appendix B. The master equation solution

The time evolution of the characteristic function in the decoherence model (3) with expressions (4), (5), and (6), the following functions appear after explicit calcu-

lations

$$\Gamma(t) = 2 \int_0^t \gamma(s) ds \quad (\text{B.1a})$$

$$\Delta_\Gamma(t) = e^{-\Gamma(t)} \int_0^t e^{\Gamma(s)} \Delta(s) ds \quad (\text{B.1b})$$

$$\Delta_{co}(t) = e^{-\Gamma(t)} \int_0^t e^{\Gamma(s)} \Delta(s) \cos[2\omega_0(t-s)] ds, \quad (\text{B.1c})$$

$$\Delta_{si}(t) = e^{-\Gamma(t)} \int_0^t e^{\Gamma(s)} \Delta(s) \sin[2\omega_0(t-s)] ds, \quad (\text{B.1d})$$

$$\Pi_{co}(t) = e^{-\Gamma(t)} \int_0^t e^{\Gamma(s)} \Pi(s) \cos[2\omega_0(t-s)] ds, \quad (\text{B.1e})$$

$$\Pi_{si}(t) = e^{-\Gamma(t)} \int_0^t e^{\Gamma(s)} \Pi(s) \sin[2\omega_0(t-s)] ds. \quad (\text{B.1f})$$

The explicit expression of the coefficients above depends on both the reservoir spectral density and the temperature. In order to find the analytic expression of the covariance matrix (10), we need to apply definition (3) and the properties of the Gaussian characteristic function to Eq. (9). To do so, we find the analytical expressions of the covariance matrices at time t can be written as

$$A_t = A_0 e^{-\Gamma} + \begin{pmatrix} \Delta_\Gamma + (\Delta_{co} - \Pi_{si}) & -(\Delta_{si} - \Pi_{co}) \\ -(\Delta_{si} - \Pi_{co}) & \Delta_\Gamma - (\Delta_{co} - \Pi_{si}) \end{pmatrix}, \quad (\text{B.2})$$

$$C_t = \begin{pmatrix} c e^{-\Gamma} \cos(2\omega_0 t) & c e^{-\Gamma} \sin(2\omega_0 t) \\ c e^{-\Gamma} \sin(2\omega_0 t) & -c e^{-\Gamma} \cos(2\omega_0 t) \end{pmatrix}. \quad (\text{B.3})$$

References

- [1] M. A. Nielsen, I.L. Chuang, *Quantum Computation and Quantum Information*, (Cambridge University Press, Cambridge, 2000)
- [2] R. Horodecki, P. Horodecki, M. Horodecki, and K. Horodecki, *Rev. Mod. Phys.* **81**, 865 (2009).
- [3] D. F. Walls and G. J. Milburn, *Quantum Optics* (Springer, Berlin, Heidelberg, 1994).
- [4] H.-P. Breuer and F. Petruccione, *The Theory of Open Quantum Systems* (Oxford University Press, Oxford, 2002).
- [5] U. Weiss, *Quantum Dissipative Systems*, (World Scientific, Singapore, 2008).
- [6] G. Lindblad, *Commun. Math. Phys.* **48**, 119 (1976).
- [7] W. H. Zurek, *Rev. Mod. Phys.* **75**, 715 (2003).
- [8] B. L. Hu, J. P. Paz, and Y. Zhang, *Phys. Rev. D* **45**, 2843 (1992).
- [9] A. Imamoglu, *Phys. Rev. A* **50**, 3650 (1994).
- [10] B. M. Garryway, *Phys. Rev. A* **55**, 2290 (1997).
- [11] B. M. Garryway, *Phys. Rev. A* **55**, 4636 (1997).
- [12] L. Mazzola, S. Maniscalco, J. Piilo, K.-A. Suominen, and B. M. Garryway, *Phys. Rev. A* **79**, 042302 (2009).
- [13] L. Mazzola, S. Maniscalco, J. Piilo, K.-A. Suominen, and B. M. Garryway, *Phys. Rev. A* **80**, 012104 (2009).

- [14] R. Hartmann and W. T. Strunz, *Phys. Rev. A* **101**, 012103 (2020).
- [15] A. S. Holevo and R. Werner, *Phys. Rev. A* **63**, 032312 (2001).
- [16] A. Serafini *et al.*, *J. Opt. B Quantum Semiclassical Opt.* **7**, R19 (2005).
- [17] M. Ban, *J. Phys. A* **39**, 1927 (2006); *Phys. Lett. A* **359**, 402 (2006).
- [18] H. McAnaney *et al.*, *J. Mod. Opt.* **52**, 935, 0950 (2005).
- [19] S. Maniscalco, S. Olivares, and M. G. A. Paris, *Phys. Rev. A* **75**, 062119 (2007).
- [20] J. H. An, M. Feng, and W. M. Zhang, arXiv:0705.2472.
- [21] K. -L. Liu and H.-S. Goan, *Phys. Rev. A* **76**, 022312 (2007).
- [22] J. H. An and W. M. Zhang, *Phys. Rev. A* **76**, 042127 (2007).
- [23] J-H. An, Y. Yeo, W-M Zhang, and C. H. Oh, arXiv:0811.1309.
- [24] M. G. A. Paris, *J. Opt. B*, **4**, 442 (2000).
- [25] A. Serafini, F. Illuminati, M. G. A. Paris and S. De Siena, *Phys. Rev. A* **69**, 022318 (2004).
- [26] S. L. Braunstein and P. van Loock, *Rev. Mod. Phys.* **77**, 513 (2005).
- [27] R. Vasile, S. Olivares, M. G. A. Paris and S. Maniscalco, *Phys. Rev. A* **67**, 062324 (2009).
- [28] R. Vasile, P. Giorda, S. Olivares, M. G. A. Paris and S. Maniscalco, *Phys. Rev. A* **82**, 012312 (2010).
- [29] R. Vasile, S. Maniscalco, M. G. A. Paris, H.-P. Breuer and J. Piilo, *Phys. Rev. A* **84**, 052118 (2011).
- [30] P. Haikka, T. H. Johnson, and S. Maniscalco, *Phys. Rev. A* **87**, 010103(R) (2013).
- [31] M. Bina, F. Grasselli, and M. G. A. Paris, *Phys. Rev. A* **97**, 012125 (2018).
- [32] A. W. Chin, S. F. Huelga, M. B. Plenio, *Phys. Rev. Lett.* **109**, 233601 (2012)
- [33] C. Benedetti, F. S. Sehdaran, M. H. Zandi, and M. G. A. Paris, *Phys. Rev. A* **97**, 012126 (2018).
- [34] F. Albarelli, M. A. C. Rossi, D. Tamascelli, and M. G. Genoni, *Quantum* **2**, 110 (2018).
- [35] F. S. Sehdaran, M. Bina, C. Benedetti, M. G. A. Paris, *Entropy* **21**, 486 (2019).
- [36] D. Tamascelli, C. Benedetti, H.-P. Breuer, and M. G. A. Paris, *New J. Phys.* **22**, 083027 (2020).
- [37] F. Gebbia, C. Benedetti, F. Benatti, R. Floreanini, M. Bina, and M. G. A. Paris, *Phys. Rev. A* **101**, 032112 (2020).
- [38] A. Candeloro and M. G. A. Paris, *Phys. Rev. A* **103**, 012217 (2021).
- [39] Z-Z Zhang and W. W, *Phys. Rev. Res.* **3**, 043039 (2021).
- [40] R. Vasile, S. Olivares, M. G. A. Paris and S. Maniscalco, *Phys. Rev. A* **83**, 042321 (2011).
- [41] B. Bylicka, D. Chruściński and S. Maniscalco, *Scientific Reports*, **4**, 5720 (2014).
- [42] C. H. Bennett, D. P. DiVincenzo, J. A. Smolin and W. K. Wootters, *Phys. Rev. A* **54**, 3824 (1996).
- [43] G. Giedke, M. M. Wolf, O. KruÅger, R. F. Werner, and J. I. Cirac, *Phys. Rev. Lett.* **91**, 107901 (2003).
- [44] P. Marian and T. A. Marian, *Phys. Rev. Lett.* **101**, 220403 (2008).
- [45] B.-H. Liu and L. Li and Y.-F. Huang and C.-F. Li and G.-C. Guo and E.-M. Laine and H.-P. Breuer and J. Piilo, *Nat. Phys.* **7**, 931 (2011).
- [46] J.-S. Tang and C.-F. Li and Y.-L. Li and X.-B. Zou and G.-C. Guo and H.-P. Breuer and E.-M. Laine and J. Piilo, *Europhys. Lett.* **97**, 10002 (2012).
- [47] F. Intravaia, S. Maniscalco, and A. Messina, *Phys. Rev. A* **67**, 042108 (2003).
- [48] W. K. Wootters, *Phys. Rev. Lett.* **80**, 2245?2248 (1998).
- [49] T. Yu and J. H. Eberly, *Phys. Rev. Lett.* **93**, 140404 (2004); *Science* **323**, 598 (2009).
- [50] M. P. Almeida, F. de Melo, M. Hor-Meyll, A. Salles, S. P. Walborn, P. H. S. Ribeiro, and L. Davidovich, *Science* **316**, 579 (2007).
- [51] B. Bellomo, R. LoFranco, and G. Compagno, *Phys. Rev. Lett.* **99**, 160502 (2007); *Phys. Rev. A* **77**, 032342 (2008).
- [52] J.-S. Xu, C.-F. Li, M. Gong, X.-B. Zou, C.-H. Shi, G. Chen, and G.-C. Guo, *Phys. Rev. Lett.* **104**, 100502 (2010).
- [53] S. Maniscalco, F. Francica, R. L. Zaffino, N. L. Gullo, and F. Plastina, *Phys. Rev. Lett.* **100**, 090503 (2008).
- [54] B. Bellomo, R. L. Franco, S. Maniscalco, and G. Compagno, *Phys. Rev. A* **78**, 060302(R) (2008).
- [55] S. John and J. Wang, *Phys. Rev. Lett.* **64**, 2418 (1990).
- [56] S. John and T. Quang, *Phys. Rev. A* **50**, 1764 (1994).
- [57] B. Teklu, *et al* (in preparation).
- [58] J. S. Prauzner-Bechcicki, *J. Phys. A* **37**, L173 (2004).
- [59] R. Alicki, M. Horodecki, P. Horodecki, and R. Horodecki, *Phys. Rev. A* **65**, 062101 (2002).
- [60] M. Abramowitz, *Handbook of Mathematical Functions*, edited by I. A. Stegun Dover Publication, New York, (1965.)